

# Formation of regular symmetric shells under non-equilibrium condition

Jef Wagner and Roya Zandi

*Department of Physics and Astronomy, University of California, Riverside, California 92521, USA*

Many studies have shown that the icosahedral symmetry adopted by most spherical viruses is the result of free energy minimization of a generic interaction between virus proteins. Remarkably, we find that icosahedral and other highly symmetric structures observed both in vitro and equilibrium studies of viral shells can readily grow from identical subunits under non equilibrium conditions. Our minimal model of virus assembly shows that structures of small shells are basically determined by the spontaneous curvature almost independently of the mechanical properties of the protein subunits.

The formation of complex ordered structures from simple identical units is of special interest in many areas of material science and biology [1–3]. Among all the biological systems, the simplicity and highly symmetric shape of viral shells with diameters ranging from 20 to 120 nm have in particular attracted the attention of physicists for many decades [3–9]. The simplest viruses are made of a genome encapsulated in a protein shell called the capsid. Quite remarkably, under many circumstances, the capsid assembles spontaneously around its genome or other negatively charged cargos to form viral shells identical to those seen in vivo [10–14]. Despite the importance of engineered virus like particles in gene and drug delivery and other biomedical technologies, the mechanisms and factors that control the structure and stability of shells and more specifically viral capsids made of identical building blocks are just beginning to be understood.

There have been many studies investigating the equilibrium shapes of shells formed from identical subunits under external constraints [3, 6–8, 14–16]. The simple case of spherical colloids or circular disks constrained to reside on the surface of a sphere reveals that stability of formed shells depends strongly on the number of assembly subunits and interactions between them. For example, the solutions of the optimal packing problem of  $N$  identical hard disks on the surface of a sphere, known as Tammes problem, reveal the presence of a number of local maxima in the plot of the sphere coverage vs.  $N$  number of disks. The structures characterized by "Magic Numbers",  $N = 12, 24, 32, 44, \dots$  corresponding to the local maximum coverage often have higher symmetry than their neighboring structures [7].

A different set of magic numbers appear when minimizing the free energy of the  $N$  identical disks interacting through Leonard Jones potential. Remarkably some of these magic numbers and their associated shells coincide with the number of capsomers (protein multimers) in structures displaying icosahedral symmetry, a characteristic of viral capsids. Magic numbers corresponding to non-icosahedral shells with octahedral and cubic symmetries also appeared in Monte Carlo simulations of disks sitting on the surface of a sphere [6, 7], consistent with the structures observed in vitro virus assembly experi-

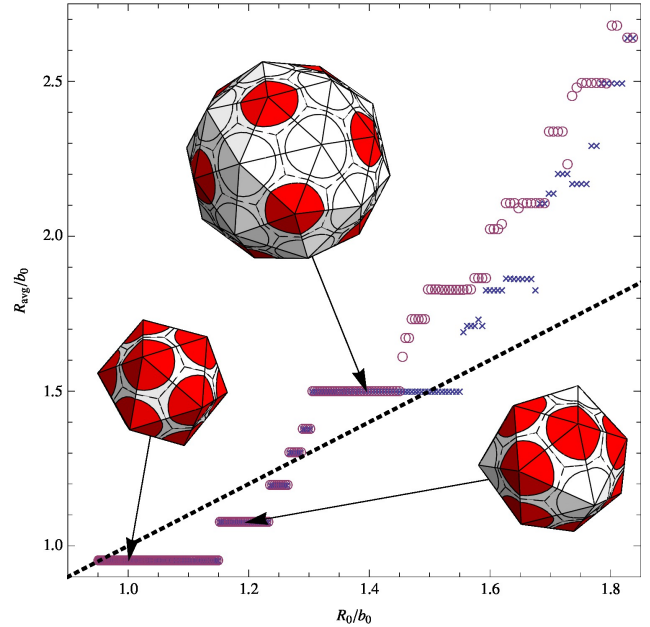


FIG. 1: Plot of the measured average radius of the closed shells  $R_{\text{avg}}$  versus the spontaneous radius of curvature  $R_0$ . The circles and triangles represent individual shells grown with  $\bar{k} = 0.2$  and  $\bar{k} = 5$ , respectively. The step-like nature of the plot for small values of radius of curvature shows the magic numbers corresponding to the number of triangular subunits in shells. Three representative capsids are shown for the first second and sixth step. The average radius is defined as the average distance of the vertices from the center of mass. The solid line has a slope of 1, and shows that very small shells have smaller radii compared to the spontaneous radius of curvature, but larger shells have larger radius than the spontaneous radius of curvature. It is worth noting that the first and sixth steps, which extend over the widest range of parameter space correspond to the shells with icosahedral symmetry.

ments. Quite interestingly, the same magic numbers and structures were observed in the Monte Carlo simulations of the self-assembly of cone-shaped particles with attractive interactions [3].

While equilibrium studies explain the appearance of icosahedral symmetry in viral capsids as the result of free energy minimization of a simple system of interacting

particles through a generic potential, the growth mechanism and kinetic pathway of virus assembly is still under intense research. This is mainly due to the fact that during the assembly process, most intermediate states are transient and thus difficult to analyze experimentally [17–20]. To this end, computer simulations have been used to elucidate the underlying physical principles governing the pathway growth and assembly of viral shells [5, 16, 21–26].

In this letter, we investigate the growth of a shell by sequentially adding subunits that connect together with a local hexagonal symmetry. While defect free stacks of hexagonal layers in the 3 dimensional space can easily grow from interacting Leonard Jones particles under non-equilibrium conditions, a closed shell requires the formation of 12 defects with local fivefold rotational symmetry (pentamers). In symmetric shells the position of pentamers with respect to each other is precise, *i.e.*, the symmetry can be readily broken if one pentagon is slightly misplaced. One would then expect that the assembly of highly symmetric icosahedral shells proceed reversibly. In fact, most previous studies and simulations were done assuming the process of assembly is completely reversible, the switching between pentamers and hexamers can easily take place when necessary [9, 13, 21, 22, 24, 27].

Despite the sensitivity of the symmetry of shells to the exact location of pentamers, under many experimental conditions the self-assembly of perfect icosahedral virus capsids is robust and efficient. The robustness of the process raises the question of whether a fully reversible assembly path is necessary for the formation of icosahedral viruses. To this end, we developed a simple model to investigate the assembly of viral shells with the minimum set of rules for irreversible growth. In each irreversible step of growth we follow the minimum energy path assuming that the protein-protein interaction is weak enough that protein subunits do not aggregate immediately, each protein explores the free energy landscape and attach to a place in the growing edge in which it maximizes the number of intermolecular bonds. The structures produced by such a model could be completely different from minimum free energy structures as during our growth process once a pentamer or hexamer is formed, it can no longer dissociate.

Unexpectedly, we found that the shells under non-equilibrium conditions grow to the structures associated with the magic numbers observed in equilibrium studies observed in Ref. [6]. In particular, we obtained the structures with icosahedral symmetry corresponding to  $T = 1$  and  $T = 3$  with  $T$  a structural index for icosahedral viral shells that can assume certain integer values such that the number of monomers in a capsid is  $60T$  [4]. Figure 1 shows the average radius of the shell obtained in our studies vs. spontaneous radius of curvature of the protein subunits. As illustrated by the stair step feature in the figure, for small spontaneous radius of curvatures we ob-

tained only a discrete set of small closed shells. The two largest steps correspond to the  $T = 1$  and  $T = 3$  icosahedral shells, while the other structures are more sensitive to the spontaneous radius of curvature. We also find that the structure of the symmetric shells is very robust and only weakly depends on the mechanical properties of proteins.

According to our studies, the symmetry of viral shell is not induced by the complex shape of the protein subunits or other complex biological mechanisms. The combined effects of small spontaneous radius of curvature of protein subunits and the local interaction between capsomers due to the elastic stress imposed by the growing shell result in the assembly of structures with *global* symmetry following *local* free energy minimization path.

To study the kinetic pathways of the shell growth, we employ trimeric protein subunits, represented as equilateral triangles, see Fig. 2. In the model, the growth proceeds through the irreversible addition of the triangular subunits to the exterior edges of the incomplete shell. After the addition of each subunit, the elastic sheet is allowed to relax and find its minimum energy configuration. The 2-dimensional shell is treated as a bond network built from triangles, where each triangle corresponds to the smallest subunit of the shell. The energy of the shell can then be separated into the bond stretching and bending energies [5, 8]. The stretching energy comes from deforming the subunits from the preferred shape of an equilateral triangle, and is modeled by considering each bond as a linear spring with spring constant  $k_s$ . The stretching energy is then simply a sum of the deformation energy over all triangles

$$E_s = \sum_i \sum_{a=1}^3 \frac{k_s}{2} (b_i^a - b_0)^2. \quad (1)$$

where  $i$  indexes the triangular subunits,  $b_0$  is the equilibrium length of the bonds, and  $b_i^a$  is the length of the  $a^{\text{th}}$  bond in the  $i^{\text{th}}$  subunit. The bending energy results from the deviation of local radius of curvature from the preferred one and is calculated by summing over all neighboring pairs of triangular subunits

$$E_b = \sum_{\langle ij \rangle} k_b (1 - \cos(\theta_{ij} - \theta_0)), \quad (2)$$

where  $\langle ij \rangle$  indexes pairs of joined subunits,  $k_b$  is the torsional spring constant, and  $\theta_0$  is the preferred angle between two subunits determined by the spontaneous radius of curvature  $R_0$ . The angle between neighboring subunits,  $\theta_{ij}$ , is defined by the relation  $\cos \theta_{ij} = \hat{n}_i \cdot \hat{n}_j$ , where  $\hat{n}_i$  is the normal vector for the  $i^{\text{th}}$  subunit.

The capsid is assumed to grow along the minimum free energy path in that at each growth step a new subunit is added to the growing edge of the shell such that it maximizes the number of neighbors at the vertices of newly

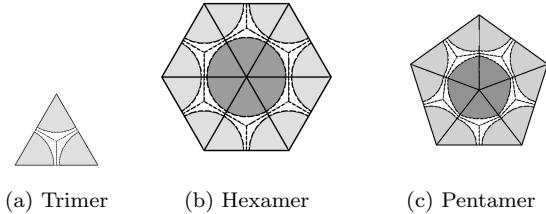


FIG. 2: (a) A basic triangular subunit. As a model for a viral capsid shell, each subunit is made up of three copies of a capsid protein represented by a wedge. When the triangular subunits bond edge to edge in a triangular lattice, each vertex with six subunits will represent a hexamer and with five subunits a pentamer.

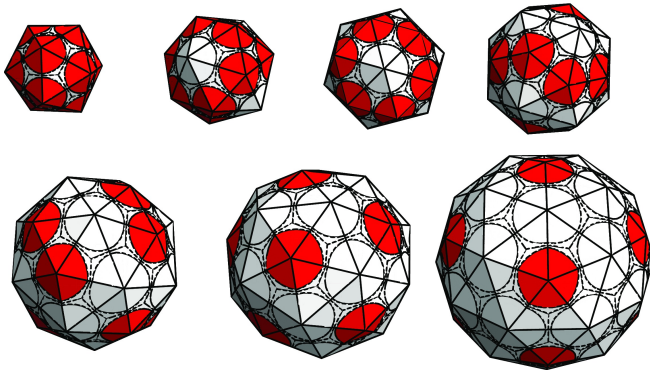


FIG. 3: The six small symmetric shells obtained for small spontaneous radius of curvatures  $R_0$ . The shells contain from the upper left 20, 28, 36, 44, 50, 60 and 80 triangular subunits, or 12, 16, 20, 24, 27, 32 and 42 capsomers (pentamers or hexamers) respectively. These shells exhibit icosahedral, tetrahedral,  $D_{6h}$  dihedral,  $D_{2h}$  dihedral,  $D_{3d}$  dihedral, icosahedral, and  $D_{5h}$  dihedral symmetry respectively. With the exception of the largest shell, the formation of these small shells is robust, and appears to be independent of relative stiffness  $\bar{k}$ .

accreted subunit. In the case of equivalent positions, the location with the smallest angles between the unbound edges of the new subunit and neighboring edges of the growing shell is chosen. If a vertex on the edge of growing shell has already 5 triangles attached then the assembly could proceed in the two different ways: (i) joining the two neighboring edges without adding a subunit and forming a pentamer, or (ii) inserting a new subunit and constructing a hexamer. The choice between forming a pentamer or a hexamer is made based on which configuration induces a total lower energy in the elastic sheet.

Many shells were grown following the locally minimum energy pathway for different values of dimensionless parameters  $\bar{k} = \frac{k_b}{k_s b_0^2}$  and  $R_0/b_0$  with  $R_0$  the preferred radius of curvature. The minimization of the elastic energy of the shell is done numerically using a non-linear conjugate gradient method[28]. The results of our numerical anal-

ysis are presented in Fig. 1, which shows the average size of the shell  $R_{\text{avg}}$  (defined as the radius of gyration of the vertices) versus the spontaneous radius of curvature  $R_0$  both in units of the equilibrium size of the subunit  $b_0$ . The red circles and blue  $\times$ s in the figure represent a shell with  $\bar{k} = 5$  and  $\bar{k} = 0.2$ , respectively. As it is clearly illustrated in Fig. 1, for smaller spontaneous radius of curvatures only a discrete set of shells grew. These shells are highly symmetric and contain 20, 28, 36, 44, 50, and 60 triangular subunits, which are related to the structures with 12 pentamers and 0, 4, 8, 12, 15, and 20 hexamers respectively. The structures corresponding to these magic numbers are illustrated in Fig. 3. The shells with 20 and 60 trimers are in particular highly symmetric, corresponding to  $T = 1$  and  $T = 3$  icosahedral structures of viral shells.

Quite amazingly, as shown in Fig. 1 for both  $\bar{k} = 5$  and  $\bar{k} = 0.2$ , changes in the spontaneous radius of curvature either have no impact on the size and symmetry of the shells, or creates a drastic effect by preventing or promoting the formation of a pentamer leading to an entirely new structure. This effect is more pronounced for  $T = 1$  and  $T = 3$  icosahedral structures in which for a relatively long range of spontaneous curvature the size of the shells does not increase despite an increase in the spontaneous radius curvature. Indeed the largest plateaus in Fig. 1 correspond to the structures with icosahedral symmetry. We emphasize here that in the simulations, the total number of subunits in the shell is a variable, *i.e.*, the size of the assembled shells is basically dictated with the spontaneous curvature of protein subunits at small  $R_0$ . Figure 1 also reveals that as  $R_0$  increases the uniform stair-step pattern breaks down and the size of the shells starts to grow along with an increase in  $R_0$ .

The small shells all display a high degree of symmetry despite the non equilibrium assembly path because of the interplay between spontaneous radius of curvature and response of the elastic triangular network to local stresses. A regular icosahedron made up of 20 triangular subunits corresponds to a radius of curvature of  $R_0/b_0 = 0.915$ , and sheet made of only hexamers will be perfectly flat corresponding to  $R_0/b_0 = \infty$ . For the range of  $R_0$  studied ( $0.915 < R_0/b_0 < 4.0$ ) the introduction of a pentamer creates too much local curvature while the introduction of a hexamer will induce too little curvature. Depending which capsomer caused more stress we found that the local distortion tended to discourage the formation of similar capsomer in the vicinity of each others. It is this effective repulsion that causes the symmetric structures observed in the shells. Small spontaneous radius of curvature ( $R_0/b_0 < 1.3$ ) favored pentamers while hexamers repelled leading to the smaller shells with tetrahedral and dihedral symmetries. Larger  $R_0/b_0$ , on the other hand, favored hexamers while pentamers repelled resulting in the 60 subunit shell with icosahedral symmetry.

As we increased the radius of spontaneous curvature

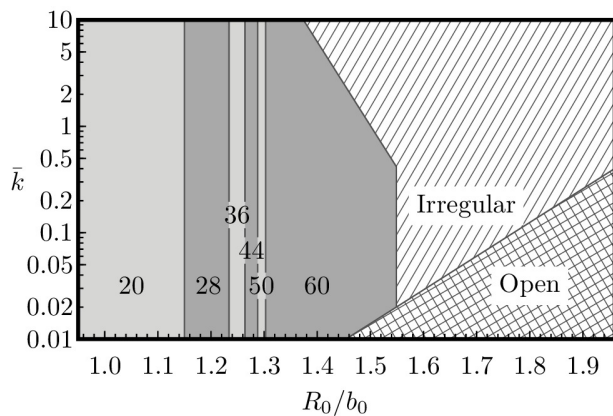


FIG. 4: Two dimensional phase diagram as a function of dimensionless spontaneous radius of curvature  $R_0/b_0$  and the dimensionless stiffness coefficient  $\bar{k}$ . The light and dark shaded regions correspond to the small symmetric magic number shells formed. The hashed region corresponds to larger closed irregular (non-symmetric) closed capsids, and the cross hatched region corresponds to the structures with zero Gaussian curvature.

beyond to that of a  $T = 3$  structure, we observed one other highly symmetric structure: a shell constructed from 80 subunits (see Fig. 3), the exact same size as a  $T = 4$  icosahedral shell. We call these shells pseudo  $T = 4$  shells because each hemisphere of the shell is identical to that of a  $T = 4$  but the distance between two pentamers on different hemispheres is not optimized. This indicates that the forces between pentamers is not long ranged enough to promote the formation of larger symmetric shells. In addition, unlike all the other highly symmetric shells the formation of the pseudo  $T = 4$  shells is not robust and depends sensitively on both  $R_0$  and  $\bar{k}$ .

As the spontaneous curvature continues to grow, creation of pentamer imposes more and more stress on the shell and at some point depending of the value of  $\bar{k}$  there is a transition from  $T = 3$  icosahedral shells to tubular or larger irregular shells as seen in Fig. 4. The phase diagram presented in Fig. 4 shows the type of shell formed for parameters ranging from  $\bar{k} = 0.01$  to  $\bar{k} = 2$  and from  $R_0/b_0 = 0.915$  to  $R_0/b_0 = 2.0$ . The figure emphasizes that for a wide range of values of spontaneous curvature and  $\bar{k}$ , the structures with icosahedral symmetry are dominant over all the other shapes. While the smaller shells reliably grow over a finite range of spontaneous curvatures independent of  $\bar{k}$ , Fig. 4 shows that the quantity  $\bar{k}$  does have a noticeable impact on the structure of shells with larger spontaneous radius of curvature. For large values of  $R_0/b$  the smaller values of  $\bar{k}$  lead to open tubes with no pentamers formed but for larger values of  $\bar{k}$  irregular shells without any symmetry are obtained. Large values of  $\bar{k}$  mean that the bending modulus is much larger than the stretching modulus, and that it is energet-

ically cheaper to change the shape of the subunits than it is to change the angle between neighboring subunits. In this regime larger spheroidal shells lacking any global symmetry tend to grow.

For large values of spontaneous radius of curvature we were indeed able to obtain similar results to the work of Hicks and Henley[5] and Levandovsky and Zandi[29, 30] both of which used slightly different variants of the model studied in this work. For larger spontaneous radius of curvatures, we obtain mostly irregular capsids with many of the larger capsids displaying defects identical to those observed in Ref. [5]. For large shells pertinent to retroviral shells and a fixed value of  $\bar{k}$ , we found a similar behavior to that seen in Ref. [29], *i.e.*, as spontaneous radius of curvature increases, the type of capsids formed changes from the irregular spheroidal capsids to larger irregular capsids often elongated including the cone shaped structure to finally tube shaped capsids.

In summary we used a minimal simple non-equilibrium model to study 2-D crystalline shell growth. We found that large spontaneous curvatures between subunits lead to the growth of small highly symmetric shells with exactly 20, 28, 36, 44, 50, or 60 subunits. While in hexagonal flat sheets, the disclinations (pentamers) repel each other, in this work we showed that high curvature of small shells made of an elastic triangular network promotes formation of pentamers and prevents assembly of hexamers, see the first plateau corresponding to  $T = 1$  structure in Fig. 1. As the spontaneous curvature between the protein subunit decreases, we found that the formation of hexamers becomes energetically less costly though; nevertheless they repel each other to alleviate the energetic costs of distortion. For larger spontaneous curvature, hexamer-hexamer repulsion disappears and pentamers starts to repel each other like disclinations in a flat hexagonal sheets. This repulsion is nevertheless short ranged, which can explain why larger viruses need scaffolding proteins or other mechanisms to form shells with icosahedral symmetry.

Quite amazingly, the magic numbers obtained in our studies correspond to the minima of free energy observed in equilibrium simulations of interacting Leonard Jones disks covering a sphere[6]. Most interestingly among all the magic number structures, the shells with exactly 20 and 60 subunits, over the largest range of curvatures and the ratio of bending to stretching modulus, form shells with icosahedral symmetry. While it has been widely accepted that the striking symmetry of viral capsids is a consequence of free energy minimization of a generic potential, this work shows that small highly symmetric shells can be reliably formed under non equilibrium conditions. Understanding the mechanisms and assembly pathways of formation of highly symmetric robust shells could have significant impact in the development of antiviral therapies and in design of novel biomimetic materials.

The authors would like to thank Gonca Erdemci-Tandogan for many helpful discussions. This work was supported by the National Science Foundation through Grant No. DMR-1310687.

- 
- [1] V. N. Manoharan, M. T. Elsesser, and D. J. Pine, *Science* **301**, 483 (2003).
  - [2] C. Li, X. Zhang, and Z. Cao, *Science* **309**, 909 (2005).
  - [3] T. Chen, Z. L. Zhang, and S. C. Glotzer, *Langmuir* **23**, 6598 (2007).
  - [4] D. L. D. Caspar and A. Klug, *Cold Spring Harbor Symp. Quant. Biol.* **27**, 1 (1962).
  - [5] S. D. Hicks and C. L. Henley, *Phys. Rev. E* **74**, 031912 (2006).
  - [6] R. Zandi, D. Reguera, R. F. Bruinsma, W. M. Gelbart, and J. Rudnick, *PNAS* **101**, 15556 (2004).
  - [7] R. F. Bruinsma, W. M. Gelbart, D. Reguera, J. Rudnick, and R. Zandi, *Phys Rev Lett* **90**, 248101 (2003).
  - [8] J. Lidmar, L. Mirny, and D. R. Nelson, *Phys Rev E* **68**, 051910 (2003).
  - [9] M. F. Hagen and D. Chandler, *Biophys J* **91**, 42 (2006).
  - [10] R. D. Cadena-Nava, M. Comas-Garcia, R. F. Garmann, A. L. N. Rao, C. M. Knobler, and W. M. Gelbart, *J Virol* **86**, 3318 (2012).
  - [11] P. Ni, Z. Wang, X. Ma, N. C. Das, P. Sokol, W. Chiu, B. Dragnea, M. Hagan, and C. C. Kao, *J. Mol. Biol.* **419**, 284 (2012).
  - [12] H. K. Lin, P. van der Schoot, and R. Zandi, *Phys Biol* **9**, 066004 (2012).
  - [13] A. Zlotnick, *J. Mol. Biol.* **241**, 59 (1994).
  - [14] A. Siber, R. Zandi, and R. Podgornik, *Phys Rev E* **81**, 051919 (2010).
  - [15] R. Twarock, K. ElSawy, A. Taomina, and L. Vaughan, *J Theo Biol* **252**, 357 (2008).
  - [16] A. Lague, D. Reguera, A. Morozov, J. Rudnick, and R. Bruinsma, *J Chem Phys* **136**, 184507 (2012).
  - [17] A. Borodavka, R. Tuma, and P. G. Stockley, *PNAS* **109**, 15769 (2012).
  - [18] Y. P. Ren, S. M. Wong, and L. Y. Lim, *J Gen Virol* **87**, 2749 (2006).
  - [19] F. D. Sikkema, M. Comellas-Aragones, R. G. Fokkink, B. J. M. Verduin, J. Cornelissen, and R. J. M. Nolte, *Org Biomol Chem* **5**, 54 (2007).
  - [20] Y. F. Hu, R. Zandi, A. Anavitarte, C. M. Knobler, and W. M. Gelbart, *Biophys J* **94**, 1428 (2008).
  - [21] R. Schwartz, P. W. Shor, P. E. Prevelige, Jr., and B. Berger, *Biophys. J.* **75**, 2626 (1998).
  - [22] H. D. Nguyen, V. S. Reddy, and C. L. Brooks III, *Nano Lett* **7**, 338 (2007).
  - [23] P. L. Freddolino, A. S. Arkhipov, S. B. Larson, A. McPherson, and K. Schulten, *Structure* **14**, 437 (2006).
  - [24] D. C. Rapaport, *Phys Rev E* **70**, 051905 (2004).
  - [25] M. F. Hagen, *Adv Chem Phys* **155** (2013), (in press).
  - [26] A. Luque, R. Zandi, and D. Reguera, *PNAS* **107**, 5323 (2010).
  - [27] R. Schwartz, R. L. Garcea, and B. Berger, *Virol.* **268**, 461 (2000).
  - [28] W. T. Vetterlin and B. P. Flannery, Numerical Recipies in C - The Art of Scientific Computing (Cambridge University Press, 1992), 2nd ed., chapter 10, section 6.
  - [29] A. Levandovsky and R. Zandi, *Phys. Rev. Lett.* **102**, 198102 (2009).
  - [30] Z. Yu, M. J. Dobro, C. L. Woodward, A. Levandovsky, C. M. Danielson, V. Sadrin, J. Shi, C. Aiken, R. Zandi, T. J. Hope, et al., *J Mol Biol* **425**, 112 (2013).